Macromolecules **1994,** *27,* 2270–2275

Polymer Diffusion in a Layered Structure of Poly(vinyl pentanal acetal) Langmuir–Blodgett Films Studied by the Interlayer Energy-Transfer Method

Takanori Hayashi, Tsuyoshi Okuyama, Shinzaburo Ito, and Masahide Yamamoto*

Division of Polymer Chemistry, Graduate School of Engineering, Kyoto University, Sakyo-ku, Kyoto 606, Japan

Received August 31, 1993; Revised Manuscript Received January 12, 1994●

ABSTRACT: The layered structure of Langmuir–Blodgett (LB) films of poly(vinyl pentanal acetal) (PVPe) has been investigated by the interlayer energy transfer from energy donor to acceptor moieties labeled to the polymer chain. The spatial order of multilayers was irreversibly disordered and mixed by the thermal treatment. The thermal relaxation clearly occurred at temperatures higher than the glass transition temperature. Theoretical calculations based on Förster kinetics were applied to this phenomenon, which was successfully represented by assuming a Gaussian distribution of chromophores in the direction normal to the layer plane. The fitting with the experimental data allowed us to evaluate the diffusion constant of polymer segments on the order of 10^{-16}–10^{-18} cm^2/s and the apparent activation energy of 150 kJ/mol. The energy-transfer method could probe the diffusion process of polymer segments in the ultrathin LB films.

Introduction

The Langmuir–Blodgett technique is an effective method to fabricate artificial molecular assemblies. It enables one to control the thickness of the layers by modifying the chain length of amphiphilic molecules and to arrange the multilayer structures by changing the substance in a molecular level. It also may enable fabrication of a highly ordered film with molecular orientation. In the LB film, one can expect to observe new aspects of chemical, physical, electrical, and biological processes. Over the past few decades, a considerable number of studies have been made on LB films.[1-3]

In the field of photophysics and photochemistry, Kuhn et al. have studied fundamental photophysical processes.[4] They realized that basic photoprocesses such as energy transfer and electron transfer can be controlled by the nanoscale structure assembled by LB multilayers. In their studies, the Förster theory[5] for the excitation energy transfer successfully represented the real systems. This means that the reverse is also possible; the layered structure of LB films could be probed by the energy transfer using fluorescent probes.

Until recently, studies on LB films have been made primarily on amphiphilic molecules, such as long-chain fatty acids. For the development of functional LB films, the understanding about the layered structure is essential. For example, IR studies,[6-9] electron microscopic studies,[7] and X-ray diffraction studies[10-13] have been performed to analyze the structure of LB film. The thermal stability of LB films is also an important research subject from the view of fundamental and application standpoints.[6,8-13] Naselli et al. investigated the thermal changes of arachidate LB monolayer assemblies by infrared spectroscopy.[8] They found a two-step melting process, and a pretransitional disordering of the hydrocarbon tails was observed prior to the melting point.

Recently, to improve the stability of LB films, polymer LB films have been investigated extensively.[14-23] Ringsdorf et al. studied the structural stability of LB films prepared from macrolipids which consists of two-chain surfactants interconnected by hydrophilic polymer chains.[17] The X-ray reflection measurement indicated that the thermal stability was improved markedly by adjustment of the molecular flexibility. Rabolt et al. also investigated the stability of polymeric LB film by polarized infrared spectroscopy.[19] The hydrophobic side chain attached to a hydrophilic main chain showed a high degree of orientation and it was disordered by heating, but it mostly recovered the orientation during the cooling process. Although X-ray scattering is a powerful tool for crystalline materials,[17,20] it is not appropriate for determining the structure of LB films made from the amorphous polymers.

We have been studying the structural relaxation and stability of the amorphous polymer LB films by the fluorescence method. Energy transfer to acceptor molecules reduces the emission probability of donor molecules. The transfer efficiency is determined by the distance between donor and acceptor, which can be controlled by spacing layers of LB films. Sensitive detection is possible even for the weak fluorescence from a monolayer containing fluorescent probes with a content of only a few percent.[24] By using this method, the aging effect of the layered structure[25] and the thermal relaxation of the structure under elevated temperatures[26] have been investigated in our laboratory.

In this study, we examined the diffusion process of polymer segments in the amorphous polymer LB films at a constant temperature. A theoretical calculation for the relaxation processes based on Förster kinetics[5] was applied to the experimental results in order to evaluate the diffusion coefficient quantitatively.

Experimental Section

Materials. Poly(vinyl pentanal acetal) (PVPe) and its derivatives were synthesized by acetalization of commercial poly(vinyl alcohol) (PVA, Wako Chemicals, dp = 2000) with pentanal and chromophoric aldehydes, according to the procedure of Ogata et al.[18] PVA powder (0.5 g), pentanal, and chromophoric aldehyde were mixed in 10 mL of chloroform containing two drops of hydrochloric acid. The reaction mixture was stirred for 24 h at 40 °C. PVA powder dissolved in the solution as the acetalization proceeded. After the reaction, the solution was diluted with 40 mL of chloroform and poured into 1 L of methanol containing a trace amount of sodium hydroxide. The polymer was purified by reprecipitation from benzene into methanol three times and then freeze-dried from benzene solution in vacuo. The chemical structures of the resulting polymers are shown in Chart 1.

● Abstract published in *Advance ACS Abstracts,* March 15, 1994.

0024-9297/94/2227-2270$04.50/0

Chart 1

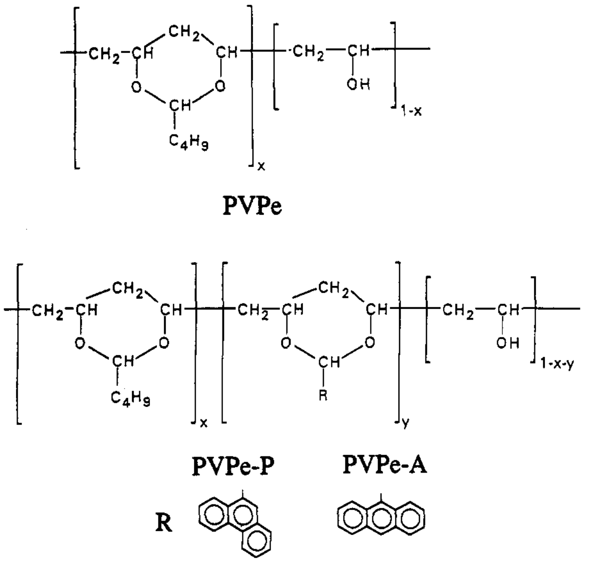

Table 1. Compositions of Synthesized Polymers and Glass Transition Temperatures

samples	x (%)	y (%)	$1-x-y$ (%)	T_g (°C)
PVPe	66	0	34	54
PVPe-P	65	8	27	77
PVPe-A	62	2	36	64

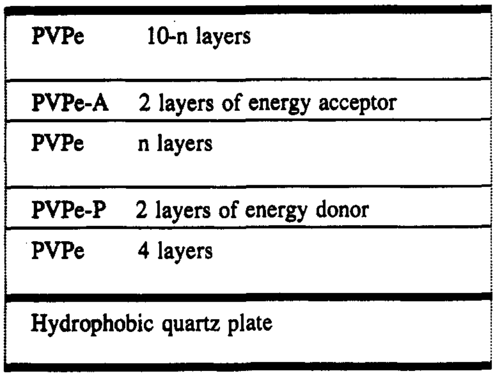

Figure 1. Schematic illustration of the multilayer structure of the PVPe LB films for the energy-transfer measurement. The figure n means the number of spacing layers: 0, 4, and 8.

Three kinds of PVPe were prepared: unlabeled PVPe for the spacing and protection layer, phenanthrene-labeled polymer (PVPe-P) for the energy-donating layer, and anthracene-labeled polymer (PVPe-A) for the energy accepting layer. Table 1 presents the compositions of pentanal unit (x) and chromophoric unit (y) which were determined from the elemental analysis and UV absorption spectra.

Sample Preparation. Pure water for the subphase was ion-exchanged, distilled, and then finally passed through a purification system (Barnstead Nanopure II). A benzene–methanol (9:1) solution of each polymer (0.01 wt %) was spread on pure water at 19 °C in a Teflon-coated trough. The surface film was compressed at a rate of 10 mm/min and transferred vertically onto a substrate at 20 mN/m for PVPe, 17.5 mN/m for PVPe-P, and 18 mN/m for PVPe-A.

A nonfluorescent quartz plate (10 mm × 40 mm) was used as a substrate for the fluorescence measurements. It was cleaned in sulfuric acid containing a small amount of potassium permanganate, dipped in 10% hydrogen peroxide solution, and then washed with water repeatedly. To make the quartz plate hydrophobic, it was soaked in a toluene solution of trimethylchlorosilane (10%) for 30 min. Under these conditions, a good transfer ratio was obtained in both the up and down modes, yielding a Y-type built-up film.

Figure 1 illustrates the structure of the LB films for energy-transfer measurements. The sample films were fabricated on a quartz plate in the following sequence: (1) four layers of PVPe for the precoating layers, (2) two layers of PVPe-P for the energy donating layers, (3) n layers (n = 0, 4, 8) of PVPe for the spacer between the donating layers and the accepting layers, (4) two layers of PVPe-A for the energy-accepting layers, (5) (10 − n) layers of PVPe for the protecting layers. To fix the composition of the film, the total number of layers was kept constant to be 18 layers by adjusting the number of the protecting layers. Therefore, sample films which have different spacing layers between the donor and acceptor layers but the same compositions of PVPe, PVPe-P, and PVPe-A can be obtained. The thickness of each layer is estimated to be 0.9 nm.[18] These are abbreviated as PVPe-n where n is the number of spacing layers.

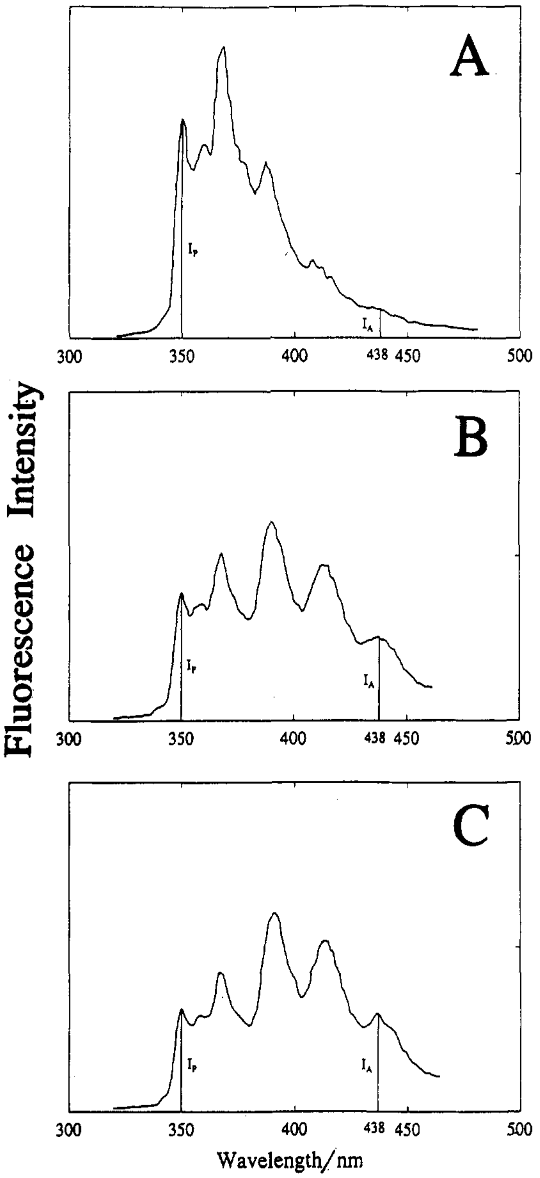

Figure 2. Spectral change of PVPe-8 films with time at a constant temperature, 60 °C: (A) initial stage, (B) after 1 h, (C) after 3 h. The excitation wavelength is 298 nm.

Measurements. UV absorption spectra were measured by a Shimadzu UV-200S spectrophotometer. The glass transition temperature (T_g) was obtained from differential scanning calorimetry (Rigaku Thermoflex DSC-8230). The fluorescence spectra were recorded by a Hitachi 850 fluorescence spectrophotometer equipped with a thermoregulated sample chamber. Heating and cooling rates were fixed to be 0.5 °C/min in the range 20–100 °C. A personal computer was used for the calculation of energy-transfer efficiency on the way of the relaxation process.

Results and Discussion

To probe the structural relaxation of the PVPe LB films, energy-transfer efficiencies between phenanthrene (P) and anthracene (A) layers were measured. The donor chro-

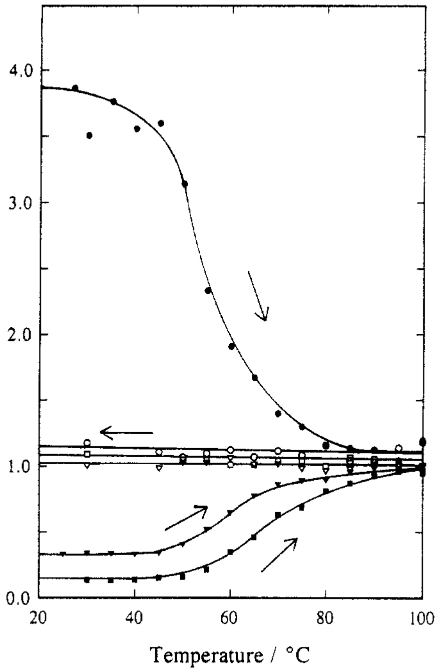

Figure 3. Effect of heating on the energy transfer efficiency of PVPe-*n* LB films: (○) PVPe-0, (▽) PVPe-4, (□) PVPe-8. Closed symbols indicate the values for the heating process, and open symbols those for the cooling process.

mophore P was slectively excited at 298 nm, and the transfer efficiency was evaluated using the fluorescence intensity ratio I_A/I_P on the spectrum, where I_A is the intensity of A emission at 438 nm and I_P is that of P at 350 nm. This method enables one to detect a small change in the distances between P and A chromophores, without considering the errors of intensity measurements among samples.

Figure 2 shows an example of spectral change of PVPe-8 sample at a constant temperature: 60 °C. A drastic change of the spectrum was observed, indicating thermal relaxation of the layered structure at the elevated temperature.

Figure 3 shows the thermal stability of PVPe-*n* films by plotting the ratio I_A/I_P as a function of temperature. The energy-transfer efficiency was measured at every 5 °C in both the heating and cooling process. The closer the distance between P and A, the higher the energy-transfer efficiency observed, resulting in a larger value of I_A/I_P, as seen in PVPe-4 and PVPe-8. On the contrary, the ratio I_A/I_P decreases when P and A begin to separate from each other, as seen in PVPe-0 which has a contact pair of P and A layers at the beginning. In both cases, thermal relaxation of the layers could be observed at temperatures above 50 °C. Compared with poly(vinyl octanal acetal) (PVO), the changes start at higher temperatures. It is probably due to the difference in T_g between PVO and PVPe, being 25 and 54 °C, respectively. The films were completely disordered when the temperature rose to 100 °C. After heating the film up to 100 °C, the ratio I_A/I_P reached a plateau region and kept its value even when the temperature decreased. Therefore, this thermal relaxation process can be regarded as an irreversible process. Moreover, the energy-transfer efficiencies of all samples showed similar values between 0.9 and 1.1 regardless of the number of spacer layers at the initial stage.

Figure 3 provides us a qualitative but general view of the phenomenon. To make a quantitative discussion on the diffusion process of the polymer segments, the energy-transfer efficiency was examined for PVPe-0, PVPe-4, and PVPe-8 and the ratio I_A/I_P was monitored as a function of time at constant temperatures between 40 and 80 °C (Figure 4).

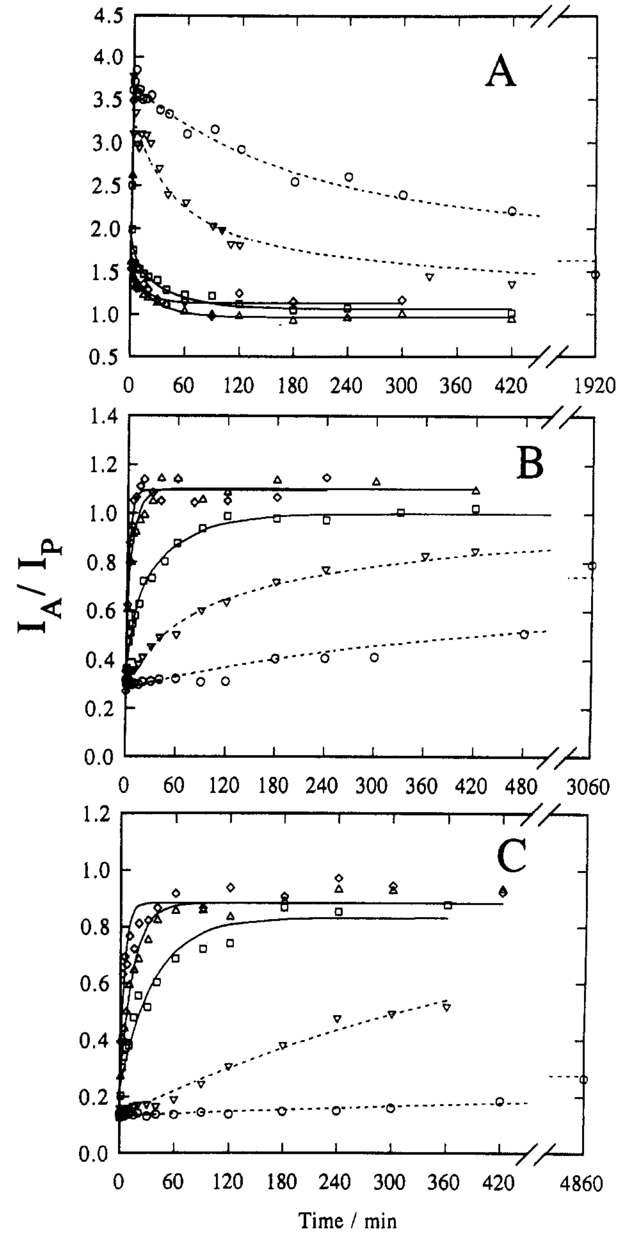

Figure 4. Energy-transfer efficiencies as a function of time at different temperatures for (A) PVPe-0, (B) PVPe-4, and (C) PVPe-8: (○) 40 °C, (▽) 50 °C, (□) 60 °C, (△) 70 °C, (◇) 80 °C.

The energy transfer efficiency of PVPe-0 which had no spacing layers decreased with time as shown in Figure 4A. From this experiment, it is obvious that P and A chromophores diffuse to the surrounding layers and consequently are separated from each other compared with the initial state. On the other hand, P and A in PVPe-4 and PVPe-8 tend to approach each other compared with the initial state as shown in Figure 4B,C. The initial slope of the I_A/I_P curves is increased, with the increase of temperature owing to the rapid relaxation. Above 60 °C, all three samples reached a plateau region, the I_A/I_P value being around 0.9–1.1. A cast film which consisted of the same components as the LB samples were prepared on a quartz plate by a spin-coating method. The ratio I_A/I_P of the cast film was found to be 1.07, which is quite similar to the equilibrium value of LB films after heating. From these results, we conclude that the layered structure of LB films was completely disordered and mixed through the thermal treatment.

The movement of chromophores in the LB films was simulated by a modeling of diffusion process. The energy-transfer efficiency of a pair of chromophores is given by the following equations:

$$T_e = k_T/(k_D + k_T) \qquad (1)$$

$$k_D = 1/\tau_D \qquad (2)$$

$$k_T = (1/\tau_D)(r_0/r)^6 \qquad (3)$$

where k_D is the fluorescence emission probability of excited donor in a unit time, k_T is the probability of Förster-type energy transfer per unit time, τ_D is the unquenched lifetime of donor, r is the distance between donor and acceptor, and r_0 is the critical transfer radius at which donor has an equal probability of energy transfer to other decay processes (2.12 nm).[27] Equations 4 and 5 are derived from eq 1. In the case of plural donors and acceptors, energy-transfer efficiencies are determined by the following procedures. Firstly, taking plural acceptors into consideration, $f(r)$ is added up for all acceptors as follows:

$$T_e = 1/[1 + f(r)^{-1}] \qquad (4)$$

$$f(r) = (r_0/r)^6 \qquad (5)$$

$$T_e = 1/\{1 + [1/\textstyle\sum f(r)]\} \qquad (6)$$

Then, the average of T_e for all donors is calculated:

$$T_e = \langle 1/\{1 + [1/\textstyle\sum f(r)]\}\rangle \qquad (7)$$

To estimate the diffusion rate of chromophores by structural relaxation, a Gaussian function, $P(x)$ was employed as a model of chromophore distribution in the direction of the film thickness (plane normal):

$$P(x) = (c_0/\sigma\sqrt{2\pi})\exp(-x^2/2\sigma^2) \qquad (8)$$

where x is a displacement of a chromophore from the distribution center, c_0 is the concentration of chromophore, and σ^2 is the variance of distribution, which is related to the diffusion constant D as follows:

$$\sigma^2 = 2Dt \qquad (9)$$

To calculate eq 7 quantitatively, we employed the following two approaches.

(1) Calculation by an Approximate Equation. Unfortunately, the analytical form of eq 7 cannot be obtained for a Gaussian distribution of both P and A. Therefore, an approximate equation was derived under an assumption that each chromophore is placed on a layer, considering the population in a Gaussian form by eq 8. This means that the displacement x is given by an integer, which represents the number of layers from the substrate. Figure 5 shows a schematic illustration of the thermal relaxation process.

We assumed that the nearest A from a certain P predominantly determines its energy-transfer efficiency. From this point of view, energy-transfer efficiency is given as follows:

$$T_e = \int_{r_1}^{\infty} 2\pi rc\exp(-\pi r^2 c)\{1/[1 + 1/g(r)]\}\,dr \qquad (10)$$

$$g(r) = f(r) + \int_{r}^{\infty} 2\pi rcf(r)\,dr \qquad (11)$$

where c is the concentration in a given layer, r is the distance between P and A chromophores, and r_1 is the excluded distance of P and A due to their molecule size. We employed r_1 = 0.6 nm from the limiting area of acetal unit: 0.36 nm^2. The probability that the nearest acceptor appears at r from the center can be represented by $2\pi rc\exp(-\pi r^2 c)$. The influence of acceptors farther than the nearest one must be small. Therefore, the contribution to the energy-transfer efficiency was taken into account by the second term of eq 11, which represents the sum of energy-transfer rates to A's appeared simply with the presence probability: $2\pi rc$. Using these equations, the energy-transfer efficiency T_e was calculated for various distributions.[28] The results were plotted against variances σ^2 in Figure 7.

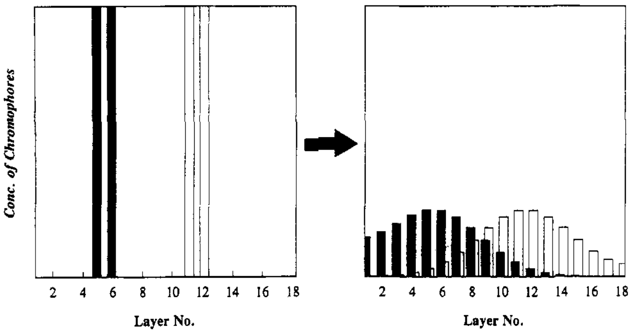

Figure 5. Schematic illustration for the thermal relaxation process of the layered structure.

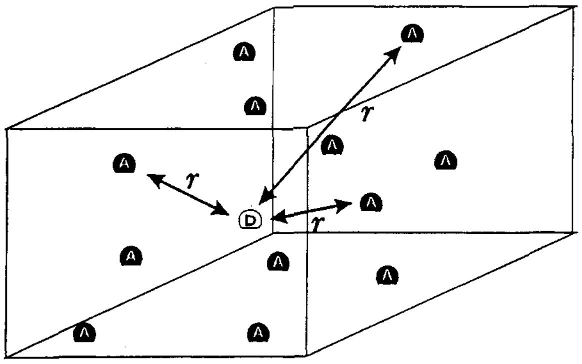

Figure 6. Schematic illustration of the model for the numerical calculation by Monte Carlo method. D represents phenanthrene chromophore, and A represents anthracene chromophore. The distance between donor and acceptor is denoted by r.

(2) Numerical Calculation by Monte Carlo Method. Another calculation using the Monte Carlo method was also carried out. The coordinates of acceptors are determined by using random numbers within the space of the film thickness, keeping a Gaussian distribution in the axis normal to the plane. Donors are also placed with a Gaussian distribution produced by random numbers. The sum of energy-transfer rates from an arbitrary donor i to all acceptors is calculated by eq 12, where r_{ij} is the distance between donor i and acceptor j. Figure 6 shows the schematic illustration of the numerical calculation. The decay curve of the donor is calculated by

$$k_{Ti} = (1/\tau_0)\sum_j (r_0/r_{ij})^6 \qquad (12)$$

$$I_{Di}(t) \propto \exp(-t/\tau_0 - k_{Ti}t) \qquad (13)$$

Then the average of all donors is obtained by

$$I_D(t) = (1/n_D)\sum_i I_{Di}(t) \qquad (14)$$

The decay curve is integrated for calculating fluorescence

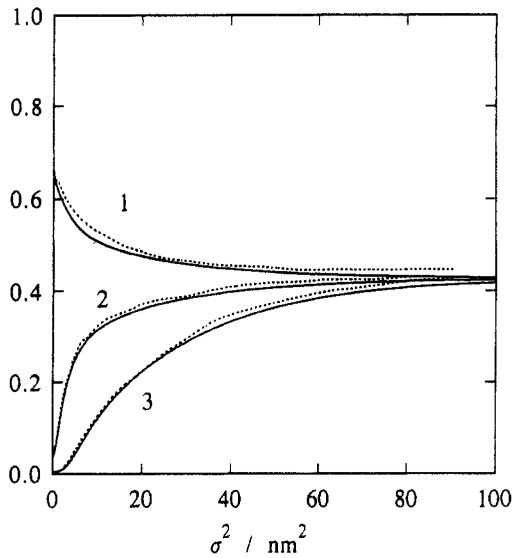

Figure 7. Calculated energy-transfer efficiency as a function of variance for (1) PVPe-0, (2) PVPe-4, and (3) PVPe-8, respectively; solid lines represent the calculation by an approximate equation and broken lines represent the numerical calculation by Monte Carlo method.

intensity I under the steady-state excitation condition as follows:

$$I = \int_0^\infty I_D(t)\,dt \tag{15}$$

T_e is evaluated by the following equation:

$$T_e = (I_0 - I)/I_0 \tag{16}$$

where I_0 is the intensity of phenanthrene chromophore without energy transfer.

Figure 7 shows the results of both calculations. These two theories show good agreement over a wide range of variance σ^2, and the features of these curves are quite similar to those in Figure 4. Now, it becomes possible to fit the experimental data, $T_{e,expt}$ with these theoretical curves $T_{e,calc}(\sigma^2)$ as follows:

$$T_{e,expt} = kT_{e,calc}(\sigma^2) \tag{17}$$

$$\sigma^2 = 2Dt + \sigma_0^2 \tag{18}$$

where k is the correction factor for the amplitude, and σ^2 in eq 9 is modified taking into account the initial dispersion, σ_0^2. We obtained the diffusion constant (D) of each samples which has a different number of spacers. Table 2 shows the best-fit values of D, k, and σ_0^2 using the least-squares fitting method. Owing to the experimental condition, it was difficult to neglect errors when the temperature was too high or too low. For example, the relaxation of PVPe-0 at 80 °C was too fast to get a reliable value of D, while the relaxation of PVPe-8 at 40 °C was too slow and did not reach the final state within the experimental time range. Therefore, these data are not shown in Table 2. Although there are some variations in the values of D, k, and σ_0^2 depending on the number of spacing layers, they are probably caused by the experimental restrictions.

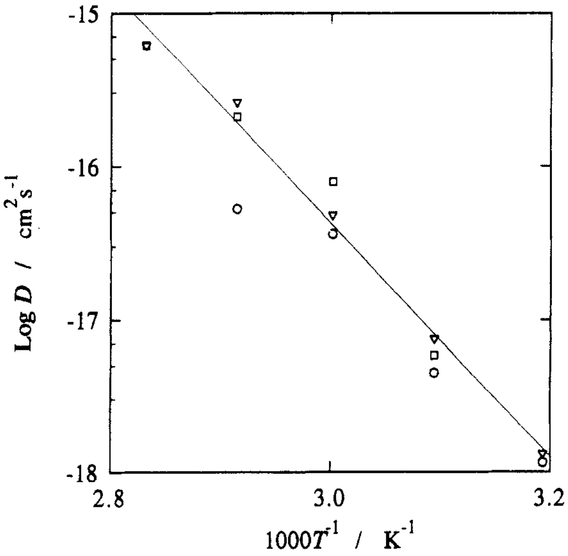

Figure 8. Arrhenius plot of diffusion constant of chromophores: (○) PVPe-0, (▽) PVPe-4, (□) PVPe-8.

The initial variance σ_0^2 shows a slight preexistent relaxation before the thermal treatment. This dispersion is partly due to the disordering after the dipping process. Especially PVPe-8 shows a large value of σ_0^2 because of the larger error arisen from the smaller I_A value. Therefore, chromophoric layers have the standard deviations σ_0 of 1.5–3.5 nm in the as-deposited LB films. It should be noted that the expected thickness of chromophoric layers is 2 nm, because these are transferred as a Y-type film, i.e., as a double layer. Figure 4 shows the calculation curves. A good agreement with experimental data was obtained.

The diffusion constant of the chromophores (D) represents the structural relaxation rate of the multilayers. For the sake of further discussion, the relation between temperatures and the diffusion coefficients was plotted in Figure 8. A linear relationship was seen between the logarithms of D and the reciprocal of temperature. From a slope of the straight line, the apparent activation energy, ΔE, for the relaxation is calculated to be about 150 kJ/mol by

$$D = D_0 \exp(-\Delta E/RT) \tag{19}$$

The D value observed is in the order of 10^{-16}–10^{-18} cm^2/s. These values are similar to the values reported for the diffusion phenomena of bulk polymers.[29–31] The polymer chains in the ultrathin LB films behave like ones in a polymer bulk, but this point must be clarified in details. Polymer diffusion in LB films is being studied by changing M_w, stereoregularity of the polymer, etc.

Table 2. Fitting Parameters for Energy-Transfer Efficiency[a]

	PVPe-0			PVPe-4			PVPe-8		
temp (°C)	k	D (10^{-18} cm^2/s)	σ_0^2 (nm^2)	k	D (10^{-18} cm^2/s)	σ_0^2 (nm^2)	k	D (10^{-18} cm^2/s)	σ_0^2 (nm^2)
40	1.2	1.2	0.051	0.7	1.3	3.6			
50	1.1	4.5	0.023	0.8	7.5	3.3	0.8	5.9	8.9
60	0.9	46.0	2.7	0.8	48.0	3.4	0.7	78.0	15.0
70	0.8	53.0	3.7	0.9	180.0	3.7	0.7	210.0	13.0
80				0.9	610.0	2.2	0.7	620.0	14.0

[a] k is the correction factor for the amplitude, D is the diffusion constant, and σ_0^2 is the initial dispersion.

Conclusion

LB films containing fluorescence probes were prepared from poly(vinyl pentanal acetal), and the thermal relaxation of the layered structure was measured by the energy transfer between phenanthrene and anthracene chromophores. This experiment enabled us to evaluate the very small diffusion coefficient of polymer segments as a function of temperature. The values observed were rather consistent with those for polymer diffusion in bulk. Furthermore, the relaxation was closely related to T_g of the sample polymers. It should be noted that fluorescence spectroscopy provides us a unique and powerful technique for probing dynamic processes occurring in the nanometer dimension.

Acknowledgment. This work was supported by a Grant-in-Aid for Developmental Scientific Research (No. 04555218), from the Ministry of Education, Science, and Culture of Japan.

References and Notes

(1) Kuhn, H. *Thin Solid Films* **1989**, *178*, 1.
(2) Ringsdorf, H.; Schmidt, G.; Schneider, J. *Thin Solid Films* **1987**, *152*, 207.
(3) Wegner, G. *Ber. Bunsen-Ges. Phys. Chem.* **1991**, *95*, 1326.
(4) Kuhn, H.; Möbius, D.; Bücher, H. In *Physical Methods of Chemistry*; Weissberger, A., Rossiter, B. W., Eds.; Wiley: New York, 1972; Vol. 1, Part 3B, p 577.
(5) Förster, Th. *Z. Naturforsch.* **1949**, *4A*, 321.
(6) (a) Hasegawa, T.; Kamata, T.; Umemura, J.; Takenaka, T. *Chem. Lett.* **1990**, 1543. (b) Umemura, J.; Kamata, T.; Kawai, T.; Takenaka, T. *J. Phys. Chem.* **1990**, *94*, 62. (c) Kamata, T.; Umemura, J.; Takenaka, T.; Koizumi, N. *J. Phys. Chem.* **1991**, *95*, 4092.
(7) Kopp, F.; Fringeli, U. P.; Mühlethaler, K.; Günthard, Hs. H. *Biophys. Struct. Mechanism* **1975**, *1*, 75.
(8) Naselli, C.; Rabolt, J. F.; Swalen, J. D. *J. Chem. Phys.* **1985**, *82*, 2136.
(9) Saperstein, D. D. *J. Phys. Chem.* **1986**, *90*, 1408.
(10) Fukui, T.; Sugi, M.; Iizima, S. *Phys. Rev. B* **1980**, *22*, 4898.
(11) Tippman-Krayer, P.; Kenn, R. M.; Möhwald, H. *Thin Solid Films* **1992**, *210/211*, 577.
(12) Richardson, W.; Blasie, J. K. *Phys. Rev. B* **1989**, *39*, 12165.
(13) Sasanuma, Y.; Kitano, Y.; Ishitani, A.; Nakahara, H.; Fukuda, K. *Thin Solid Films* **1991**, *199*, 359.
(14) (a) Schouten, A. J.; Wegner, G. *Makromol. Chem.* **1991**, *192*, 2203. (b) Arndt, T.; Schouten, A. J.; Schmidt, G. F.; Wegner, G. *Makromol. Chem.* **1991**, *192*, 2215.
(15) O'Brien, K. C.; Lando, J. B. *Langmuir* **1985**, *1*, 453.
(16) Shigehara, K.; Murata, Y.; Amiya, N.; Yamada, A. *Thin Solid Films* **1989**, *179*, 287.
(17) (a) Laschewsky, A.; Ringsdorf, H.; Schmidt, G.; Schneider, J. *J. Am. Chem. Soc.* **1987**, *109*, 788. (b) Erdelen, C.; Laschewsky, A.; Ringsdorf, H.; Schneider, J.; Schuster, A. *Thin Solid Films* **1989**, *180*, 153.
(18) (a) Oguchi, K.; Yoden, T.; Sanui, K.; Ogata, N. *Polym. J.* **1986**, *18*, 887. (b) Watanabe, M.; Kosaka, Y.; Sanui, K.; Ogata, N.; Oguchi, K.; Yoden, T. *Macromolecules* **1987**, *20*, 452. (c) Watanabe, M.; Kosaka, Y.; Oguchi, K.; Sanui, K.; Ogata, N. *Macromolecules* **1988**, *21*, 2997.
(19) (a) Schneider, J.; Ringsdorf, H.; Rabolt, J. F. *Macromolecules* **1989**, *22*, 205. (b) Schneider, J.; Erdelen, C.; Ringsdorf, H.; Rabolt, J. F. *Macromolecules* **1989**, *22*, 3475.
(20) Mumby, S. J.; Swalen, J. D.; Rabolt, J. F. *Macromolecules* **1986**, *19*, 1054.
(21) Shimomura, M.; Song, K.; Rabolt, J. F. *Langmuir* **1992**, *8*, 887.
(22) Jark, W.; Russell, T. P.; Comelli, G.; Stöhr, J. *Thin Solid Films* **1991**, *199*, 161.
(23) Naito, K. *J. Colloid Interface Sci.* **1989**, *131*, 218.
(24) Ito, S.; Kanno, K.; Ohmori, S.; Onogi, Y.; Yamamoto, M. *Macromolecules* **1991**, *24*, 659.
(25) Ohmori, S.; Ito, S.; Yamamoto, M. *Macromolecules* **1991**, *24*, 2377.
(26) Ueno, T.; Ito, S.; Ohmori, S.; Onogi, Y.; Yamamoto, M. *Macromolecules* **1992**, *25*, 7150.
(27) Berlman, I. B. *Energy Transfer Parameters of Aromatic Compounds*; Academic Press: New York, 1973.
(28) In the text, we described procedures only for the intralayer energy transfer for the sake of simplicity. When D and A locate in different planes, T_e can be calculated by a modified form of eq 10:

$$T_e = \int_0^\infty 2\pi lc \exp(-\pi l^2 c)\{1/[1 + 1/h(l)]\}\,\mathrm{d}l \tag{20}$$

$$h(l) = {r_0}^6/(l^2 + {r_2}^2)^3 + \pi c {r_0}^6/2(l^2 + {r_2}^2)^2 \tag{21}$$

where l is the distance from the center of a plane to A chromophores in the plane, and r_2 is the layer distance between donating layers and accepting layers. Equations 10 and 20 were taken into account for all layers.
(29) (a) Pekcan, Ö.; Winnik, M. A.; Droucher, M. D. *Macromolecules* **1990**, *23*, 2673. (b) Zhao, C.; Wang, Y.; Hruska, Z.; Winnik, M. A. *Macromolecules* **1990**, *23*, 4082.
(30) Yukioka, S.; Nagato, K.; Inoue, T. *Polymer* **1992**, *33*, 1171.
(31) Nealey, P. F.; Cohen, R. E.; Argon, A. S. *Macromolecules* **1993**, *26*, 1287.